



## Activated carbon produced from sugarcane bagasse waste as a low-cost dye-containing wastewater adsorbent for reactive turquoise blue removal

Siyu Li\*, Lina Wang, Xiuqin Yang, Yanwei Wang

School of Material and Chemical Engineering, Henan University of Engineering, Zhengzhou 450000, China, Tel. +86 13663843369; email: lisiyu4728@163.com (S.Y. Li), Tel. +86 13526717262; email: wln.xin@163.com (L.N. Wang), Tel. +86 13592601632; email: yangxiuqin-1297@163.com (X.Q. Yang), Tel. +86 037167717823; email: wyw0214@163.com (Y.W. Wang)

Received 11 November 2016; Accepted 2 July 2017

### ABSTRACT

Sugarcane bagasse-based activated carbon (SBAC) materials had been successfully prepared from sugarcane waste by zinc chloride activated method. Structure of the obtained materials was studied by scanning electron microscopy, X-ray diffraction and a surface area and pore size analysis method. Adsorption performances of the as-prepared materials were evaluated by a batch method on a 722 spectrophotometer. Results indicated that the obtained materials had abundant pore structure, that is, the Brunauer–Emmett–Teller surface area could be up to 1,843 m<sup>2</sup>/g and the total pore volume  $V_t$  increased with increasing activator proportion. The proportion of mesopores increased first and then decreased with increasing activator proportion. For the sample of SBAC-3, the mesoporous surface area content can be up to 52% and there was a sharp peak at 4.9 nm by quenched solid density functional theory. Adsorption experiments showed that the obtained material had good adsorption performance. The acid condition is benefit for the adsorption behaviour. The adsorption quantity of SBAC-3 increased with increasing the initial dye concentration.

*Keywords:* Biomass; Sugarcane bagasse; Activated carbon; Adsorption

### 1. Introduction

It is well known that the dye-containing wastewater is now a serious problem and has attracted much attention. Textile, leather, paper and plastic industries use dyes to decorate their products and consume volumes of water [1,2]. As a result, they generate a considerable amount of dye-containing wastewater. Dyes are synthetic aromatic water-soluble dispersible organic colourants and are toxic to aquatic flora and fauna even in relatively low concentrations. A number of authors have been studying on the toxicity of dyes and their impact on the environment [3–6].

It is difficult to remove the dyes from the effluent because the dyes are stable to light and heat and are biologically non-degradable [7]. Various treatment techniques such as reverse osmosis, electrodialysis, ultrafiltration, ion-exchange

and chemical precipitation have been used for the removal of coloured dyes from wastewater [8–13], but only that of adsorption is considered to be superior to other techniques. This is attributed to its low cost, easy availability, simplicity of design, high efficiency, easy operation and ability to treat dyes in more concentrated forms [14,15]. Nanoporous carbons are one of the most used adsorbents because of their excellent properties such as high porosity, large surface area, good conductivity and low cost [16–18]. Traditional nanoporous carbon materials are mainly prepared from non-renewable resources such as coal, coal tar, and asphalt. [19–23], which consume the non-renewable fuels. Furthermore, the properties of obtained products are poor and price is high restricted by technological conditions.

In recent years, extensive research has been undertaken to develop nanoporous carbons from alternative and economic carbon precursors. An economic carbon precursor is defined as one which is abundant in nature or is a by-product or waste and require little processing. On this

\* Corresponding author.

point, biomass has inherent advantages. Considering the factors of environmental quality, national security, agricultural production and rural development [24,25], agricultural and forestry wastes such as husks [26], straws [27], peels [28], lignin [29,30], shells [31,32] and stems [33], have received much attention recently. These wastes are mainly composed of cellulose, hemicellulose and lignin and have high carbon content, which makes it suitable for conversion into a porous carbonaceous material.

Therefore, a number of inexpensive and effective low-cost biomasses are being used to prepare nanoporous carbon for dyes removal from aqueous solutions [34–37]. China is one of the largest cane sugar producers and the plantation area of sugarcane ranked the third in the world. It will produce large amount of bagasse after the extraction of sucrose from sugarcane and the treatment and disposal of the bagasse will be a great challenge. Thus, recycling sugarcane bagasse to useful adsorption materials has great economic benefits, and their disposal pressure can be partially eased. Some investigations have reported sugarcane bagasse as an economical carbon precursor for the adsorption of heavy metal ions and dyes from aqueous solution [38–41]. In this study, sugarcane bagasse is used as carbon resource to prepare nanoporous carbons and their adsorption performance for reactive turquoise blue (TB) has been also studied.

## 2. Experimental section

### 2.1. Preparation of sugarcane bagasse-based activated carbon materials

Sugarcane bagasse, obtained from the market in Zhengzhou, China, was washed and cut into pieces. The treated sugarcane bagasse was preoxidized in a muffle furnace at 250°C under air atmosphere for 3 h. Predetermined amount activator zinc chloride ( $\text{ZnCl}_2$ ) and the oxidized sugarcane bagasse (OSB) was mixed well with a moderate amount of water. The mass ratios of  $\text{ZnCl}_2$  and OSB were 1:1, 2:1, 3:1 and 4:1. The mixture was soaked for 12 h at room temperature and then dried at 110°C. The obtained composites were carbonized and activated at 800°C for 3 h under the flowing  $\text{N}_2$ , followed by soaking in 20% hydrochloric acid (HCl). Finally, activated carbon materials were obtained after washing and drying the above samples. The as-prepared sugarcane bagasse-based activated carbon (SBAC) materials were denoted as SBAC- $x$ , where  $x$  represented the mass ratio of  $\text{ZnCl}_2$  and OSB.

### 2.2. Material characterization

The microstructure of the carbon samples was investigated by an FEI Quanta 250 scanning electron microscope (SEM), a Bruker D8 ADVANCE X-ray diffractometer (XRD) and a 2QDS-MP-30 automated surface area and pore size analyzer (Quantachrome Instruments Corporation). Prior to measurements, the sample was degassed for more than 3 h at 300°C under vacuum. The Brunauer–Emmett–Teller (BET)-specific surface area ( $S_{\text{BET}}$ ) was calculated by BET theory. The total pore volume ( $V_t$ ) was estimated from single point adsorption at a relative pressure  $P/P_0 \approx 0.99$ . The micropore surface area ( $S_{\text{mic}}$ ) was determined by t-plot theory. The pore

size distribution and density functional theory (DFT)-specific surface area was determined by quenched solid density functional theory (QSDFT).

### 2.3. Adsorption characterization

Adsorption was determined by batch method, which was simple and easy to perform. In batch method, a fixed amount of the adsorbent (0.5 g) was added to 20 mL dye solution with a certain concentration and thoroughly mixed in well-closed flasks. Then, all the flasks were allowed to stand for 120 min at 50°C. The pH values of dye solutions (1, 2, 3, 4, 5), initial dye concentration (1, 2, 3, 4 mg/mL) were evaluated in the present study. Then, the suspensions were centrifuged at 4,000 rpm for 15 min. The solutions were carefully decanted to be analyzed using a 722 spectrophotometer (Shanghai Precision & Scientific Instrument Co., Ltd.) at 528 nm, which was the maximum wavelength for reactive TB. The adsorption quantity and efficiency were calculated based on the following equations:

$$q = \frac{(C_0 - C_1)V}{m} \quad (1)$$

$$E = \frac{C_0 - C_1}{C_0} \times 100\% \quad (2)$$

where  $q$  is the amount of dye adsorbed in carbon,  $C_0$  and  $C_1$  are the initial and equilibrium concentrations of dye solutions,  $m$  is the amount of adsorbent,  $V$  is the volume of solution and  $E$  is the adsorption efficiency.

## 3. Results and discussion

### 3.1. Microstructures of the as-prepared samples

Fig. 1 is the SEM image of sugarcane bagasse. As shown in Fig. 1, the rectangular pore walls form honeycomb-shaped skeleton. The width of the honeycomb-shaped pore is about 100  $\mu\text{m}$ . The skeleton is smooth and there are a few pores

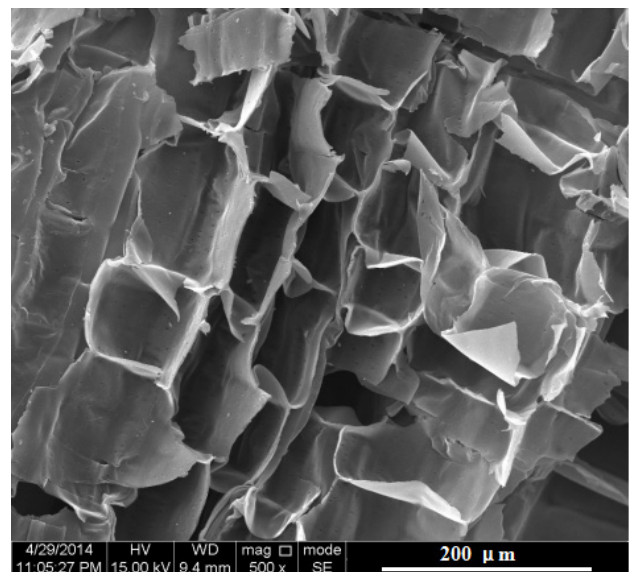


Fig. 1. SEM image of sugarcane bagasse.

in the skeleton. After activation and carbonization at 900°C, the obtained carbons have abundant cylindrical macropores, which arrange regularly in longitudinal formed carbon skeleton. The width of cylindrical macropores is about 13  $\mu\text{m}$  (Fig. 2). From Fig. 2, we can also see that the carbon skeleton split after activation (Figs. 2(a)–(c)) and collapse to pieces when activator proportion is 4:1 (Fig. 2(d)). This can be due to the activated reaction between  $\text{ZnCl}_2$  and carbon skeleton during the heat treatment.

Fig. 3 shows the XRD results of samples with different mass ratio of activator and sugarcane bagasse ( $A/B$ ). It is shown that steamed bread like 002 peaks appear at about  $23^\circ$ , which indicates that the obtained material is amorphous. In most cases, activation degree of the obtained carbon increases with increasing the activator proportion and it results in carbon skeleton collapsing and become more disorder. However, for SBAC, 002 peaks grow stronger and shift to a higher angle with increasing the activator proportion. This is because that the macroporous structures burst and the carbon skeletons stack. The carbon pieces recombine to new graphite microcrystal during high temperature treatment. There are obvious 100 peaks at about  $45^\circ$  and graphite micro-crystalline structure at about  $80^\circ$  (the insert in Fig. 3).

The  $\text{N}_2$  adsorption–desorption isotherms of the obtained carbon materials with different activator proportions are shown in Fig. 4. According to the isotherms of the samples,

$S_{\text{BET}}$ ,  $S_{\text{mic}}$ ,  $S_{\text{DFP}}$ ,  $V_p$ , and pore size distribution of the samples are obtained and the results are shown in Table 1 and Fig. 5. Results show that sugarcane bagasse-based carbons have abundant pore structure, high specific surface area and high pore volume after activation by  $\text{ZnCl}_2$ .

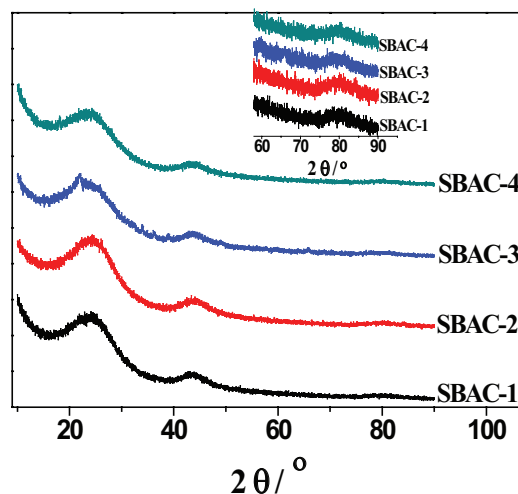


Fig. 3. XRD curves of the obtained samples.

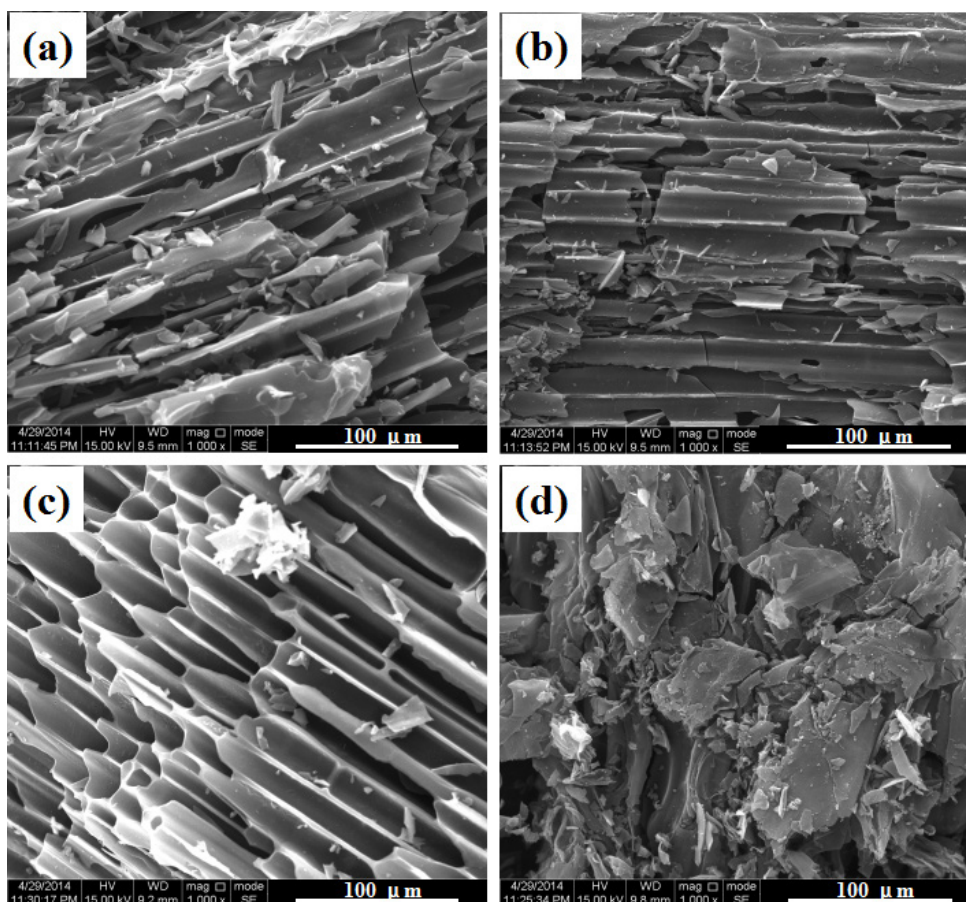


Fig. 2. SEM images of sugarcane bagasse-based activated carbons: (a) SBAC-1; (b) SBAC-2; (c) SBAC-3; (d) SBAC-4.

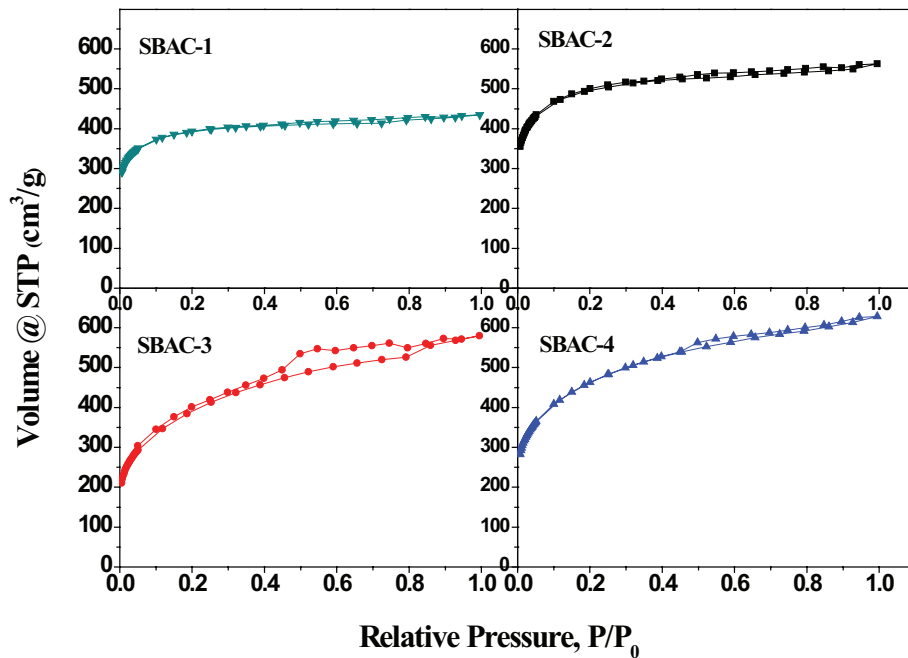


Fig. 4.  $N_2$  adsorption–desorption isotherms of the as-prepared carbon samples.

Table 1  
Pore structure parameters of the obtained samples

Sample	BET			QSDFT			$V_t$ (cm <sup>3</sup> /g)
	$S_{BET}$ (m <sup>2</sup> /g)	$S_{mic}$ (m <sup>2</sup> /g)	$S_{mic}/S_{BET}$ (%)	$S_{DFT}$ (m <sup>2</sup> /g)	$S_{mic}$ (m <sup>2</sup> /g)	$S_{mic}/S_{DFT}$ (%)	
SBAC-1	1,458	1,335	92	1,401	1,230	88	0.672
SBAC-2	1,843	1,626	88	1,717	1,424	83	0.870
SBAC-3	1,414	736	52	1,142	553	48	0.896
SBAC-4	1,663	1,040	63	1,446	919	64	0.972

It can be clearly seen from the isotherms (Fig. 4) that the adsorption amount increases clearly at low relative pressure ( $P/P_0$ ) and the adsorption occurs in the micropores. The adsorption amount increases slightly with increasing the  $P/P_0$  when activator mass ratio is relatively low and the isotherm is of type-I-B. For example, for the sample of SBAC-1, the adsorption volume increases from 300 to 434 cm<sup>3</sup>/g when  $P/P_0$  is from 0.01 to 0.99. The adsorption volume increases obviously with increasing  $A/B$  ratio and the isotherm is type-IV when  $A/B$  is 3:1. There is an obvious type-H4 hysteresis loop when  $A/B$  ratio is 3:1, which indicates that the obtained material SBAC-3 has both micropores and mesopores. Furthermore, the proportion of mesopores increases first and then decreases with the increasing  $A/B$  ratio (Table 1), which agrees well with the QSDFT pore size distribution curves (Fig. 5). When  $A/B$  is 3:1, the mesoporous surface area content is the highest and it can be up to 52% by QSDFT (Table 1).

As shown in the QSDFT curves in Fig. 5, there are obvious peaks at 1.0, 2.2 and 4.9 nm in all samples. However, there are some significant differences in the sample structure. For SBAC-1 and SBAC-2, the position and number of the peaks are almost the same in addition to peak intensity. The SBAC-2

has stronger peak intensity, which indicates that it is more porous and has the highest surface area (Table 1). For SBAC-3, the position of micropore shift to 1.3 nm and there is a peak at 3.5 nm and there is also a relatively weaker wide peak at 7.3–12.0 nm. Furthermore, the peak at 4.9 nm is very strong, which indicates that the pores are trend to mesopores. For SBAC-4, the peak intensity at 4.9 nm become weaker than that of SBAC-3 and distribution of big size pores is wider and its intensity is weaker (Fig. 5), which results in the decrease of surface area (Table 1).

Table 1 shows the BET and DFT surface area and pore volume. It is obviously seen that the obtained materials have high specific surface area. The SBAC-1 and SBAC-2 are typical microporous materials and the microporous surface area content can be up to 92% and 88%, respectively. With increasing the activator proportion, the micropores content decreases and mesopores content increases, for example, there is a sharp peak at 4.9 nm in the sample of SBAC-3. The microporous surface area content is only 52% calculated by BET and the  $S_{BET}$  is only 1,414 m<sup>2</sup>/g. However, when  $A/B = 4:1$ , the  $S_{BET}$  increases to 1,663 m<sup>2</sup>/g and microporous surface area content increases to 63% accordingly. Results calculated by QSDFT theory have the similar trends. When the

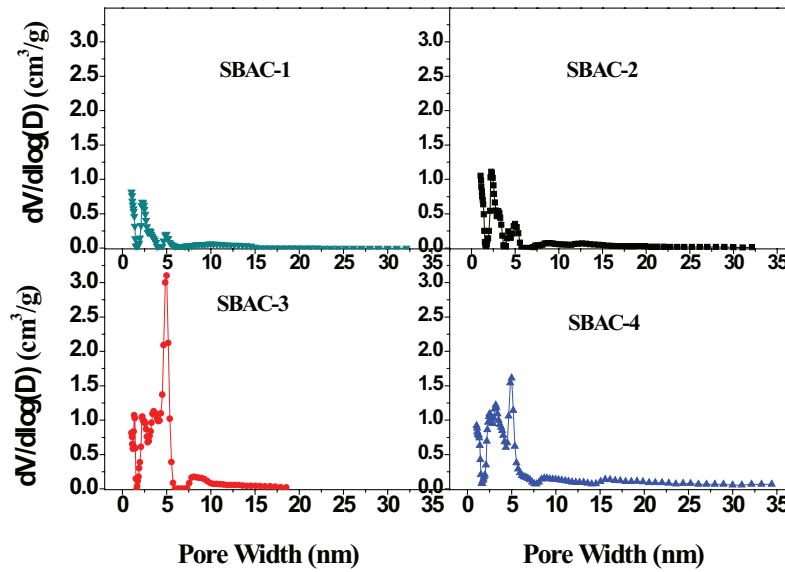


Fig. 5. QSDFT pore size distribution curves of the as-prepared carbon samples.

activator is less, the obtained materials are mainly microporous. With increasing the activator proportion, the activation degree increases correspondingly, so the specific surface area increases first. When the activator proportion increases to a certain extent, the pore size becomes larger and micropore content decreases, which results in the decrease of specific surface area. The total pore volume  $V_t$  estimated from single point adsorption at a relative pressure  $P/P_0 \approx 0.99$  increases with increasing activator proportion. This may be because that activation degree of the obtained carbon increases with increasing the activator proportion and activated reaction between  $ZnCl_2$  and carbon skeleton during the heat treatment results in the increase of pore volume.

3.2. Adsorption properties

Fig. 6 is the standard curve of reactive TB. As shown in Fig. 6, the absorbency ( $y$ ) and dye concentration ( $x$ ) of reactive TB solution have good linearization. The linearity can be described as in Eq. (3).

$$y = -0.040 + 0.694x \tag{3}$$

The initial pH value of the solution is an important process controlling parameter in adsorption [42]. The adsorption behaviour of sugarcane bagasse-based carbons on reactive TB was studied at the varying pH range of 1.0–5.0, 20 mg/mL initial dye concentration with 0.2 g adsorbent at 50°C for 2 h. Fig. 7 shows the effect of the pH value on adsorption of dye aqueous solution onto sugarcane bagasse-based carbon. Results showed that reactive TB solution got lighter immediately after the obtained material SBAC-3 was added to the solution. Furthermore, the dye solution got lighter with decreasing solution pH value. This indicated that the adsorption behaviour was easier in acid condition.

Table 2 shows the effect of initial dye concentration on the adsorption performance of reactive TB using SBAC-3. It was observed that as the initial dye concentration increased

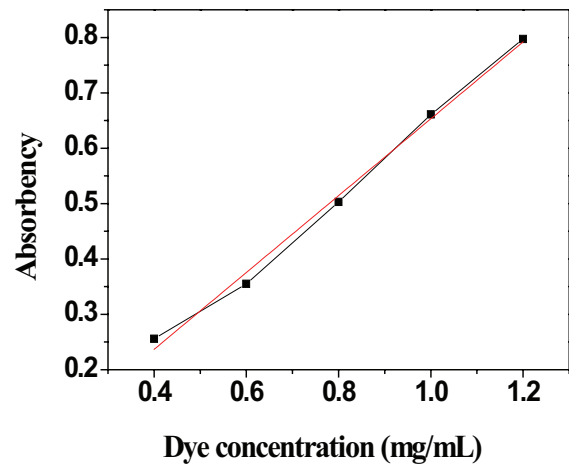


Fig. 6. Standard curve of reactive turquoise blue.

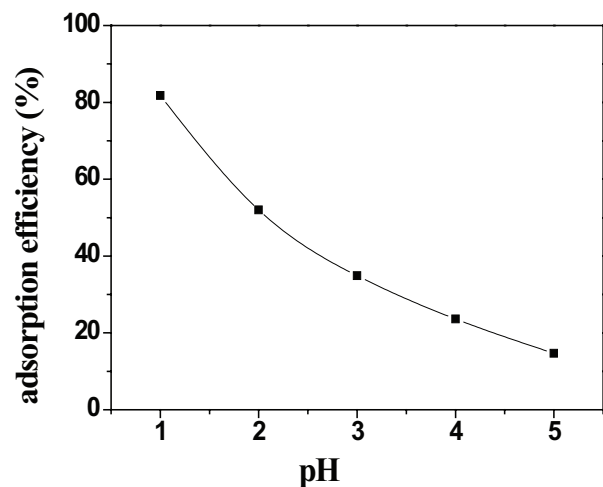


Fig. 7. The effect of pH on adsorption performance of dye aqueous solution onto sugarcane bagasse-based carbon.

Table 2  
Adsorption properties of SBAC-3 for reactive turquoise blue

Initial dye concentration, $C_0$ (mg/mL)	Absorbance (A)	Dye concentration after adsorption, $C_1$ (mg/mL)	Adsorption quantity (mg/g)	Adsorption efficiency (%)
1	0.281	0.463	21.5	53.7
2	0.665	1.016	39.4	49.2
3	1.037	1.552	57.9	48.3
4	1.701	2.509	59.6	37.3

from 1 to 4 mg/mL, the adsorption efficiency decreased from 53.7% to 37.3%. However, the adsorption capacity of SBAC-3 increased from 21.5 to 59.6 mg/g (Table 2). This is because that increasing the initial dye concentration provides a driving force to overcome all mass transfer resistances of dyes between the aqueous and solid phase.

#### 4. Conclusions

Sugarcane bagasse-based activated carbon materials had been successfully prepared from sugarcane waste by  $ZnCl_2$ -activated method. The prepared materials had abundant nanopores. XRD results showed that 002 peaks grew stronger and shifted to a higher angle with increasing the activator proportion due to the collapse of macroporous structure and the recombination of graphite microcrystal during high temperature treatment.  $N_2$  adsorption-desorption isotherm changed from type-I-B to type-IV when activator proportion was from 1:1 to 3:1 and the micropores proportion decrease from 92% to 52%. The BET surface area and total pore volume could be up to 1,843  $m^2/g$  and 0.972  $m^3/g$ , respectively. The total pore volume  $V_t$  increased with increasing activator proportion due to the increase of activation degree between  $ZnCl_2$  and carbon skeleton. The obtained material had good adsorption performance and the adsorption efficiency increased with decreasing solution pH value. The adsorption quantity of SBAC-3 increased with increasing the initial dye concentration and it increased from 21.5 to 59.6 mg/g when the initial dye concentration increased from 1 to 4 mg/mL.

#### Acknowledgements

This research was supported by the project of colleges and universities key scientific research project of Henan Province (17A430002) and Science & Technology Project of Henan Province (142102210402).

#### References

- M.R. Khan, S.I. Mozumder, A. Islam, D.M.R. PrasadM, M. Alam, Methylene blue adsorption onto water hyacinth: batch and column study, *Water Air Soil Pollut.*, 223 (2012) 2943–2953.
- P.S. Kumar, S. Ramalingam, K. Sathishkumar, Removal of methylene blue dye from aqueous solution by activated carbon prepared from cashew nut shell as a new low-cost adsorbent, *Korean J. Chem. Eng.*, 28 (2011) 149–155.
- S.Y. Li, Y. Wang, Y. Wei, J. Zeng, W.Y. Shi, Y.W. Wang, Preparation and adsorption performance of palm fiber-based nanoporous carbon materials with high specific surface area, *J. Porous Mater.*, 23 (2016) 1059–1064.
- L. Wang, Q. Li, A.Q. Wang, Adsorption of cationic dye on N,O-carboxymethyl-chitosan from aqueous solutions: equilibrium, kinetics, and adsorption mechanism, *Polym. Bull.*, 65 (2010) 961–975.
- M. Asgher, Biosorption of reactive dyes: a review, *Water Air Soil Pollut.*, 223 (2012) 2417–2435.
- S.T. Akar, A.S. Özcan, T. Akar, A. Özcanb, Z. Kaynakk, Biosorption of a reactive textile dye from aqueous solutions utilizing an agro-waste, *Desalination*, 249 (2009) 757–761.
- M.S. Chiou, G.S. Chuang, Competitive adsorption of dye metanil yellow and RB15 in acid solutions on chemically cross-linked chitosan beads, *Chemosphere*, 62 (2006) 731–740.
- G. Ciardelli, L. Corsi, M. Marucci, Membrane separation for wastewater reuse in the textile industry, *Resour. Conserv. Recycl.*, 31 (2001) 189–197.
- M.K. Purkait, A. Maiti, S. DasGupta, S. De, Removal of Congo red using activated carbon and its regeneration, *J. Hazard Mater.*, 145 (2007) 287–295.
- A. Alinsafi, M. Khemis, M.N. Pons, J.P. Leclerc, A. Yaacoubi, A. Benhammou, A. Nejmeddine, Electro-coagulation of reactive textile dyes and textile wastewater, *Chem. Eng. Process.*, 44 (2005) 461–470.
- M. Muthukumar, N. Selvakumar, Studies on the effect of inorganic salts on decolouration of acid dye effluents by ozonation, *Dyes Pigments*, 62 (2004) 221–228.
- S. Mondal, H. Ouni, M. Dhahbi, S. De, Kinetic modeling for dye removal using polyelectrolyte enhanced ultrafiltration, *J. Hazard. Mater.*, 229–230 (2012) 381–389.
- G. Gehlot, S. Verma, S. Sharma, N. Mehta, Adsorption isotherm studies in the removal of malachite green dye from aqueous solution by using coal fly ash, *Int. J. Chem. Stud.*, 3 (2015) 42–44.
- S.Y. Li, Y.W. Wang, R.W. Fu, Preparation and weak acid dark blue adsorption studies of melamine formaldehyde-based nanoporous carbon, *Proc. IMechE. Part N: J. Nanoeng. Nanosyst.*, 227 (2013) 185–189.
- V. Meshko, L. Markovska, M. Mincheva, A.E. Rodrigues, Adsorption of basic dyes on granular activated carbon and natural zeolite, *Water Res.* 35 (2001) 3357–3366.
- R.L. Tseng, F.C. Wu, R.S. Juang, Liquid-phase adsorption of dyes and phenols using pinewood-based activated carbons, *Carbon*, 41 (2003) 487–495.
- Y. Chen, C. Liu, F. Li, H.M. Cheng, Pore structures of multiwalled carbon nanotubes activated by air,  $CO_2$  and KOH, *J. Porous Mater.*, 13 (2006) 141–146.
- P.K. Malik, Use of activated carbons prepared from sawdust and rice-husk for adsorption of acid dyes: a case study of acid yellow 36, *Dyes Pigments*, 56 (2003) 239–249.
- Y. Yamashita, K. Ouchi, Influence of alkali on the carbonization process-II: carbonization of various coals and asphalt with NaOH, *Carbon*, 20 (1982) 47–53.
- L.S. Liu, Z.Y. Liu, Z.G. Huang, Z.H. Liu, P.G. Liu, Preparation of activated carbon honeycomb monolith directly from coal, *Carbon*, 44 (2006) 1598–1601.
- T. Tomko, R. Rajagopalan, M. Lanagan, H.C. Foley, High energy density capacitor using coal tar pitch derived nanoporous carbon/ $MnO_2$  electrodes in aqueous electrolytes, *J. Power Sources*, 196 (2011) 2380–2386.
- S.Y. Li, Y.R. Liang, D.C. Wu, R.W. Fu, Fabrication of bimodal mesoporous carbons from petroleum pitch by a one-step nanocasting method, *Carbon*, 48 (2010) 839–843.

- [23] E. Daguerre, A. Guillot, F. Stoeckli, Activated carbons prepared from thermally and chemically treated petroleum and coal tar pitches, *Carbon*, 39 (2001) 1279–1285.
- [24] R.C. Brown, T.R. Brown, *Biorenewable Resources-Engineering New Products from Agriculture*, 2nd ed., John Wiley & Sons, Oxford, 2014.
- [25] Y.M. Chang, W.T. Tsai, M.H. Li, Characterization of activated carbon prepared from chlorella-based algal residue, *Bioresour. Technol.*, 184 (2015) 344–348.
- [26] Y. Chen, S.R. Zhai, N. Liu, Y. Song, Q.D. An, X.W. Song, Dye removal of activated carbons prepared from NaOH-pretreated rice husks by low-temperature solution-processed carbonization and  $H_3PO_4$  activation, *Bioresour. Technol.*, 144 (2013) 401–409.
- [27] S.Y. Li, L.L. Sun, L.N. Wang, Y. Wang, Preparation and electrochemical performance of corn straw-based nanoporous carbon, *J. Porous Mater.*, 22 (2015) 1351–1355.
- [28] H. Gupta, B. Gupta, Adsorption of polycyclic aromatic hydrocarbons on banana peel activated carbon, *Desal. Wat. Treat.*, 57 (2016) 9498–9509.
- [29] Atul V. Maldhure, J.D. Ekhe, Preparation and characterizations of microwave assisted activated carbons from industrial waste lignin for Cu(II) sorption, *Chem. Eng. J.*, 168 (2011) 1103–1111.
- [30] A.M. Navarro-Suárez, J. Carretero-González, V. Roddatis, E. Goikolea, J. Ségalini, E. Redondo, T. Rojo, R. Mysyka, Nanoporous carbons from natural lignin: study of structural-textural properties and application to organic-based supercapacitors, *RSC Adv.*, 4 (2014) 48336–48343.
- [31] G.R. Kovummal, A.J. Pattayil, Coconut shell based activated carbon-iron oxide magnetic nanocomposite for fast and efficient removal of oil spills, *J. Environ. Chem. Eng.*, 3 (2015) 2068–2075.
- [32] G.G. Choi, S.J. Oh, S.J. Lee, J.S. Kim, Production of bio-based phenolic resin and activated carbon from bio-oil and biochar derived from fast pyrolysis of palm kernel shells, *Bioresour. Technol.*, 178 (2015) 99–107.
- [33] I. Lupul, J. Yperman, R. Carleer, G. Gryglewicz, Tailoring of porous texture of hemp stem-based activated carbon produced by phosphoric acid activation in steam atmosphere, *J. Porous Mater.*, 22 (2015) 283–289.
- [34] A. Demirbas, Agricultural based activated carbons for the removal of dyes from aqueous solutions: a review, *J. Hazard. Mater.*, 167 (2009) 1–9.
- [35] J.M. Dias, M.C.M. Alvim-Ferraz, M.F. Almeida, J. Rivera-Utrilla, M. Sánchez-Polo, Waste materials for activated carbon preparation and its use in aqueous-phase treatment: a review, *J. Environ. Manage.*, 85 (2007) 833–846.
- [36] B. Hu, K. Wang, L.H. Wu, S.H. Yu, M. Antonietti, M.M. Titirici, Engineering carbon materials from the hydrothermal carbonization process of biomass, *Adv. Mater.*, 22 (2010) 813–828.
- [37] M. He, Y. Sun, B. Han, Green carbon science: scientific basis for integrating carbon resource processing, utilization, and recycling, *Angew. Chem. Int. Ed.*, 52 (2013) 9620–9633.
- [38] M. Valix, W.H. Cheung, G. McKay, Preparation of activated carbon using low temperature carbonisation and physical activation of high ash raw bagasse for acid dye adsorption, *Chemosphere*, 56 (2004) 493–501.
- [39] N.K. Amin, Removal of reactive dye from aqueous solutions by adsorption onto activated carbons prepared from sugarcane bagasse pith, *Desalination*, 223 (2008) 152–161.
- [40] K.J. Cronje, K. Chetty, M. Carsky, J.N. Sahu, B.C. Meikap, Optimization of chromium(VI) sorption potential using developed activated carbon from sugarcane bagasse with chemical activation by zinc chloride, *Desalination*, 275 (2011) 276–284.
- [41] K.A. Krishnan, K.G. Sreejalekshmi, R.S. Baiju, Nickel(II) adsorption onto biomass based activated carbon obtained from sugarcane bagasse pith, *Bioresour. Technol.*, 102 (2011) 10239–10247.
- [42] H. Lata, V.V. Garg, R.K. Gupta, Removal of a basic dye from aqueous solution by adsorption using parthenium hysterophorus: an agricultural waste, *Dyes Pigments*, 74 (2007) 653–658.